Journal of Food Composition and Analysis 131 (2024) 106220

Contents lists available at ScienceDirect

Journal of Food Composition and Analysis

journal homepage: www.elsevier.com/locate/jfca

Effect of ultrasonic processing on beef tenderness in *longissimus lumborum* during aging by proteomics analysis

Sumin Gao [a,1], Zhicheng Xu [a,b,1], Hengpeng Wang [a,b,*], Anqi Xu [a], Chuanming Huan [a], Xiuyun Guo [a,b], Rui Liu [d], Peng Wu [a,b], Xiangren Meng [a,b,c,*]

[a] Key Laboratory of Chinese Cuisine Intangible Cultural Heritage Technology Inheritance, Ministry of Culture and Tourism, College of Tourism and Culinary Science, Yangzhou University, Yangzhou 225127, China
[b] Engineering Technology Research Center of Yangzhou Prepared Cuisine, Yangzhou 225127, China
[c] Chinese Cuisine Promotion and Research Base, Yangzhou University, Yangzhou 225127, China
[d] College of Food Science and Engineering, Yangzhou University, Yangzhou, 225009, China

ARTICLE INFO

Keywords:
Postmortem aging
Beef
Proteomics
Tenderness
Ultrasound

ABSTRACT

This investigation was aimed to evaluate the proteins related to beef tenderness at different aging times (1, 3, 7 d) and to explain the changes in the *longissimus lumborum* at the molecular level with ultrasound treatment. The pH value decreased significantly ($p<0.05$) with increasing aging time, and was lower in the ultrasonic group compared to the non-ultrasonic group. It indicated that ultrasound had a positive effect on tenderness by maintaining lower cooking loss, higher water-holding capacity (WHC), and higher myofibril fragmentation index (MFI), as demonstrated by the immunoblotting analysis of desmin and caspase-3. Twenty-eight proteins were identified as potential markers of tenderness. A PCA analysis confirmed the differential expression of tenderness-related proteins. Bioinformatics analysis suggested that these proteins, which were distributed in the cytoplasm, membrane, and mitochondria, were more likely to be impacted by ultrasound. Overall, the identified proteomics database of beef serves as a valuable reference for using ultrasound to enhance meat quality and reduce aging duration.

1. Introduction

As an important sensory characteristic of meat, tenderness has always been considered one of the most considerable factors for purchasers to judge the quality of meat and influence consumption (Brewer and Novakofski, 2008; Huff-Lonergan *et al.*, 2010; Kim *et al.*, 2014). Following animal slaughter, hypoxia affects animal cells and tissues, while muscular cells undergo apoptosis (Herrera-Mendez et al., 2006). This process leads to the degradation of myofibril, markedly enhancing meat tenderness. The aging and tenderization strongly promote the hydrolysis and decomposition of key proteins in muscle fibers, particularly the protein degradation of desmin. It has been established that meat tenderization is mainly affected by the increase of fragmentation of muscle structure after death (as well as other factors, such as sarcomere length and background hardness) (Goll et al., 2003). Moreover, the degradation of cytoskeleton myofibrillar protein in meat using endogenous protein hydrolysis system can significantly improve the dietary quality, such as juiciness, flavor, and tenderness (Kim et al., 2018).

Ultrasound technology is extensively used in the meat industry to improve tenderness. When the ultrasonic system operates, partial energy is converted into cavitation energy, leading to the growth and rupture of bubbles in liquid media, ultimately triggering various biological and physicochemical reactions. Ultrasound has been proven to enhance the rupture of skeletal muscle z-line and destroy organelles, like mitochondria and sarcoplasmic reticulum (Stadnik *et al.*, 2008). In fresh meat productions, this effect is generally regarded as beneficial as it can improve tenderness. Similarly, Wang et al. (2018) proposed that power ultrasound can improve the tenderness by stimulating postmortem protein hydrolysis and physically destroying myofibril structure. It has been confirmed that ultrasound can enhance the tenderness of meat and shorten the aging phase while leaving other quality parameters

* Corresponding authors at: Key Laboratory of Chinese Cuisine Intangible Cultural Heritage Technology Inheritance, Ministry of Culture and Tourism, College of Tourism and Culinary Science, Yangzhou University, Yangzhou 225127, China.
E-mail addresses: yzuwhp@163.com (H. Wang), xrmeng@yzu.edu.cn (X. Meng).
[1] These authors have contributed equally to this work.

https://doi.org/10.1016/j.jfca.2024.106220
Received 8 November 2023; Received in revised form 8 March 2024; Accepted 1 April 2024
Available online 7 April 2024

unaffected (Barekat and Soltanizadeh, 2018; Peña-González et al., 2017).

At present, new proteomics technology employed in meat science has significantly been conducive to understanding the relevance between complicated biological mechanisms and quality. Quantitative proteomics methodology provides valuable insights into the biological mechanism of meat quality traits and protein properties (Purslow et al., 2021; Shi et al., 2018; Picard and Gagaoua, 2020). Malheiros et al. (2019) investigated the influence of protein oxidation on beef tenderness by 2D-DIGE proteomics approach, and detected several potential biomarkers connected with beef tenderness. Currently, proteomics studies in meat are primarily focused on researching the protein expression variations among different meat varieties and qualities (Bax et al., 2013; Hou et al., 2020). Number of studies addressing quantitative proteomic approaches of tenderness biomarkers grew-up finding as well (Bonnet et al., 2020; Huang et al., 2020; López-Pedrouso et al., 2021). However, rarely studies evaluating the tenderness of postmortem aged beef after ultrasound treatment combined with Quantitative proteomics methodology was performed in the last years. The primary aim of this study were 1) To characterize the quality changes related to tenderness of aged beef *longissimus lumborum* by evaluating pH, color, WHC, and texture. 2) To assess the effect of ultrasound on myofibril protein by measuring myofibril fragmentation index, immunoblotting of caspase-3, and desmin. 3) To explore the mechanism of beef tenderization after ultrasonic treatment by quantitative proteomics methodology. The findings will assist in the development of suitable conditions for promoting ultrasonic technology on an industrial scale.

2. Materials and methods

2.1. Sample collection and experimental design

Muscles samples were obtained from the same farm (Wuxi Tianpeng Group Co., China) and slaughtered by a commercial slaughtering method at age of 24 months. The averaged live weight was 800 ± 20 kg. Within 30 min of the bleeding completely, *longissimus lumborum* was taken out from both sides, and transported to the laboratory for preservation under ice bag in 2 h. Each muscle was separated into 12 equal parts, each measuring 8.0 cm×6.0 cm×2.5 cm, after all visible lipids, ligaments, tendons, and connective tissues were removed. There were 72 muscle segments used, and each one was randomly assigned to one of eight treatments (two ultrasonication times×four aging periods). All samples were vacuum-packed into bags (TC-400A, Xingbei Packaging Machinery Co., China). Briefly, ultrasonic treatment (40 kHz, 200 W, 40 min) was performed while maintaining a 4°C water temperature (González-González et al., 2017). The group without ultrasound treatment was labelled "CK". These samples to be used for quality analysis were directly measured at the end of aging. Liquid nitrogen and a blender (H7d, Xiamen Hehui Electronic Technology Co., Fujian, China) were used to quickly freeze and pulverize the remaining muscle tissue. The materials were initially stored at −80°C for further biochemical analyses, such as pH, myofibril fragmentation index (MFI), and western blotting.

2.2. pH

The pH values were measured using a pH meter (Testo 205, Lenzkirch, Germany), which can be directly inserted into the muscle at various stages of aging. Standard buffer solutions with pH values of 4.00 and 6.86 were used to calibrate the electrode at the same temperature.

2.3. Color

The fresh meat surface color was measured after being unwrapped and standing for 30 min. The lightness (L^*), redness (a^*), yellowness (b^*), chroma ($C^*=(a^{*2}+b^{*2})^{0.5}$), and hue angle ($h^*$=arctan(b*/a*)) values were determined by an automatic colorimeter (CR-410, Minolta Co., Tokyo, Japan) (Li et al., 2019) set to the illiuminant C, observer angle of 2°, aperture size of 50 mm after calibrated with a standard black and white plate. The following formula (1) was used to calculate the ΔE^* value, which represented the overall difference in color between the tested sample and the original sample aging for 0 d.

$$\Delta E = \sqrt{(\Delta L^*)^2 + (\Delta a^*)^2 + (\Delta b^*)^2} \quad (1)$$

In formula (1): ΔL^*, Δa^* and Δb^*: the difference in brightness, redness, and yellowing values between each sample and the initial sample.

2.4. Shear force analysis

The shear force was carried out by the procedures of Holman et al. (2015) with slight modifications. Six replicate measurements were drilled with a diameter of 1.27 cm in a direction parallel to the beef muscle fibers. An analyzer (C-LM3B, Tianxiang Feiyu Co., Beijing.) was used to estimate the shear force immediately.

2.5. Water holding capacity and cooking loss determination

The water holding capacity (WHC) was determined using the pressurization method according to Sarabandi et al. (2018). Approximately 3.0 g of meat with the same specification (1 cm×1 cm×0.5 cm) was weighed and placed on a previously dried filter paper with two thin plastic films. The filter paper containing the meat sample was sandwiched between two plates of stainless steel, then a load of 35 kg was applied for 5 min. Meat samples were removed accurately and rapidly weighed. The weight difference was later measured in order to calculate the value of WHC, which was then stated as the formula (2) below:

$$Water\ holding\ capacity(\%) = (1 - (W_1/W_0)) \times 100 \quad (2)$$

In formula (2): W_1, the weight of meat after pressing; W_0, the total weight of meat before pressing.

The cooking loss was performed as described by Montowska and Pospiech (2013). Vacuum-packed beef *longissimus lumborum* was placed into separate cooking bags and heated to a core temperature of 75℃ before being cooked in a water bath at 80℃ for 30 min. The cooked beef samples were weighed after removing the drip when cooled to room temperature (20℃). The cooking loss (%) was determined by calculating the weight loss after cooking as the following formula (3):

$$Cooking\ loss(\%) = (1 - (W_1/W_0)) \times 100 \quad (3)$$

In formula (3): W_1, the weight of meat after cooking; W_0, the total weight of meat before cooking.

2.6. Myofibril fragmentation index determination

The myofibril fragmentation index (MFI) was carried out with some modifications according to Culler et al. (1978). Powdered beef sample (2 g) was homogenized in duplicate with 20 mL cold MFI buffer solution [100 mol/L KCl, 11.2 mmol/L K_2HPO_4, 8.8 mol/L KH_2PO_4, 1 mmol/L EDTA, 1 mmol/L $MgCl_2$, and 1 mmol/L NaN_3] for about 30 s. Samples were centrifuged (4°C, 3500 g, 20 min) two times. The supernatant was removed and 20 mL fresh cold MFI buffer was added to precipitate through eddy current resuspension. Afterwards, the above operation was repeated once. The samples were filtrated using 150 mesh gauze to remove excess connective tissue. MFI quantification was measured using a UV spectrophotometer (P1, MAPADA Instrument Co., Ltd, China) by reading the absorbance at 540 nm after correcting the sample's protein concentration to 0.5 mg/mL by adding MFI buffer. The absorbance of the mixture was then measured at 540 nm. The MFI values were calculated as 200× the sample absorbance as the following formula (4):

$$MFI = A_{540nm} \times 200 \quad (4)$$

In formula (4): $A_{540\ nm}$, the absorbance measured at 540 nm.

2.7. Western blot analysis

20 mg beef was washed twice with 3 mL phosphate buffer solution (0.01 mol/L, pH 7.2). After adding enzyme inhibitors, 100 μL lysis buffer was added to the chopped beef. It was then ground to complete lysis, centrifuged (4℃, 12,000 g, 5 min) and the supernatant was collected for determination of protein concentration with a BCA kit. A 12 % polyacrylamide separating gel and 5 % stacking gel were used to determine the desmin and caspase-3. About 10 μL of the samples were loaded onto the gel. The electrophoresis was performed at 70 V for 30 min and 90 V for 2 h. After that, the proteins on the gel were transferred to PVDF membranes at a stationary current of 200 mA for 30 or 70 min. PVDF membranes were quickly removed and placed in 5 % BSA for room temperature sealing for 2 h. Next, the membranes were incubated overnight with antibody by gentle shaking at 4℃, followed by 3 TBS-T rinses (5 min per wash). Anti-mouse and anti-rabbit HRP-conjugated antibodies (1:2000 dilution) were then incubated with the membranes at room temperature for 2 h after washing the cells in TBS-T to remove excess antibody. TBS-T was used to rinse the PVDF membrane five times (15 min per wash). The GAPDH bands were visualized serving as an internal standard. A ChemiDoc XRS gel documentation system was used to scan the membranes, and Quantity One software was used to quantify and analyze the band intensities.

2.8. Proteomics analysis

2.8.1. Protein extraction and digestion

Samples of beef *longissimus lumborum* at 1 d of aging with non-ultrasonic and ultrasonic were ground into powder using liquid nitrogen. Approximately 20 mg of powder was resuspended in 200 μL lysis buffer (4 % SDS, 100 mmol/L DTT, 150 mmol/L Tris-HCl, pH 8.0). The samples were boiled and further ultrasonicated to ensure complete lysis. Then, undissolved cellular debris were removed by centrifugation (4℃, 16,000 g, 15 min). The supernatant was collected and quantified with a BCA Protein Assay Kit (Bio-Rad, USA).

Digestion of protein was performed according to the FASP procedure described by Wiśniewski et al. (2009). The proteins were transferred to a 1.5-mL Nanosep tube (Pall Corporation, MWCO 10 K) and centrifuged (20℃, 14,000 g, 20 min) to remove the DTT. Next, 100 μL of IAA in UA buffer (0.05 mol/L) was added to block reduced cysteine residues and the samples were incubated for 20 min in darkness. Then, 200 μL of Ammonium bicarbonate buffer (100 mmol/L) was added to the beads in the filter cartridge and centrifuged (25℃, 14000 g, 15 min). Finally, trypsin was added to the sample at an enzyme-to-protein ratio of 1:50 along with 50–100 μL of Ammonium bicarbonate buffer (50 mmol/L) and incubated at 37℃ for 20 h. The peptides were collected by centrifugation, acidified with 1 % FA, and dried using a refrigerated CentriVap concentrator (Labconco, Kansas, MO). The tryptic digested peptides were ultimately desalted with C18 stage tip. The peptide concentrations were determined using the OD280 method on a Nanodrop One device.

2.8.2. LC-MS analysis

The peptides were loaded onto the C18-reversed phase column (75 μm×150 mm, 2 μm, Dr. Maisch GmbH, Ammerbuch, German) in buffer A (2 % ACN and 0.1 % FA) and separated with a linear gradient of buffer B (90 % ACN and 0.1 % FA) at a flow rate of 300 nL/min over 60 min. For MS data acquisition, the timsTOF Pro2 (Bruker) was operated in PASEF mode. The full scans were recorded from 100 to 1700 *m/z* spanning from 0.6 to 1.6 Vs/cm2 in the mobility (1/K0) dimension. The MS method was set as follows: ramp time of 100 ms, accumulation time of 2.0 ms, lock duty cycle at 100 %, capillary voltage of 1700 V, dry gas of 3 L/min, dry temperature of 180°C. Following a full MS, 10 PASEF MS/MS frames were conducted on ion-mobility separated precursors. Singly charged ions, which are fully segregated in the mobility dimension, were excluded. The threshold and target intensity were set at 1750 and 15,000 counts, respectively. The CID collision energy was set to 42 eV.

2.8.3. Bioinformatics analysis

Perseus software, Microsoft Excel, and R statistical computer software were applied to evaluate bioinformatics data (Tyanova et al., 2016). To annotate the sequences, information was taken from UniProtKB/Swiss-Prot and Gene Ontology (GO) (Ashburner et al., 2000). Enriched GO and KEGG pathways were nominally statistically significant at the level of $p<0.05$. Quantitative MS1 and qualitative MS/MS data was processed by MSFragger 3.4 and Uniprot-Bos taurus (Bovine). The MS data were analyzed for data interpretation and protein identification against the Bos taurus (Bovine) database from Uniprot (downloaded on 12/22/2022, and including 47138 protein sequences), which is sourced from the protein database at https://www.uniprot.org/taxonomy/9913. The identifying parameters were as follows: digestion enzyme, trypsin; maximum deletion cleavage, 2; main search, 6 ppm; Precursor Tolerance, 20 ppm; MS/MS tolerance, 20 ppm. Peptide-Spectral Matching and protein FDR were set to 0.01. Proteins were selected to be statistically significant with fold change (FC)>1.5 or <0.6667 (Jia et al., 2021). Construction of protein–protein interaction (PPI) networks were also conducted by using the STRING database.

2.9. Statistical analysis

A completely random design was utilized, and each measurement was independently repeated at least six times. The SPSS software (Version 23, IBM Crop., USA) was used to analyze the variables under each corresponding fitted linear mixed model (LMM). For each model, the fixed effects included treatments (ultrasonic/non-ultrasonic) and aging periods (0, 1, 3, 7 d), and the interaction between them (denoted by treatment × aging), and random residual error. The effects of ultrasound processing were examined using analyses of variance, and $p<0.05$ was regarded as statistically significant. Results were expressed as means ± standard deviations and the Origin software (Version 2021, OriginPro Corp., USA) was used to visualize. The variation in mean values was evaluated by the Duncan's multiple range test. Principal component analysis (PCA), Hierarchical clustering analysis (HCA) and partial least squares discriminant analysis (PLS-DA) were performed on protein samples using MetaboAnalyst 5.0.

3. Results and discussion

3.1. Changes in beef quality

3.1.1. pH

The pH value of beef *longissimus lumborum* (Table S1) was significantly affected ($p<0.05$) by ultrasound and aging durations. It decreased from 6.24 to 5.64 in the course of 7 days of aging, which was in line with the findings from Li et al. (2022). After slaughter, the accumulation of lactic acid produced during anaerobic glycolysis led to an immediate decrease in the pH value of all muscles, allowing for subsequent maturation processes. Compared to the sample without ultrasound treatment, the pH values of the ultrasonic group were significantly lower ($p<0.05$). This indicated that ultrasound treatment accelerated the aging process of beef *longissimus lumborum*, consequently shortening the aging time considerably.

3.1.2. Color

Significant differences were observed for lightness value (L^*), redness value (a^*), yellowness value (b^*), and chroma value (C^*) between ultrasonic and non-ultrasonic samples. During 7 days of aging, L^*

exhibited a declining tendency ($p<0.05$) in the samples, which was brought on by changes in the water scattering and migration on the surface of the meat. a^* value gradually decreased probably because of the rise in water loss, which led to an increase in myoglobin loss of beef. It could also be observed that the redness and yellowness values of the ultrasonic group were significantly lower ($p<0.05$) than those of the control group, which was mainly related to the cavitation effect of ultrasound. The cavitation effect may lead to muscle relaxation, increased absorption and swelling of muscle fibres, and partial dissolution of pigments. The color values for the ultrasonic sample generally decreased to levels similar to or lower than the initial level after 7 days of aging. C^* value is an excellent indication of the degree of oxidation of meat exposed to air since it indicates the intensity of a color and the clarity or dullness of the color. The C^* value had a significant decreased ($p<0.05$) over time in this study. The hue angle (h^*) showed a trend of change from yellow to red as increasing aging time. The ultrasonic sample's ΔE significantly decreased ($p<0.05$) from 11.68 to 1.15. Additionally, ultrasound was effective in maintaining colour stability as evidenced by the lower ΔE value of the ultrasound group. Protein oxidation and breakdown typically generated color components according to the report of Zhang et al. (2019). Thus, meat discolouration would result from a higher degree of protein oxidation and breakdown during the aging process.

3.1.3. Shear force and water-holding capacity

Table S2 displayed the results of the influence of aging time (1, 3 and 7 d) on the shear force values of the *longissimus lumborum* in Simmental cattle. As expected, the shear force value was found to be affected by aging ($P < 0.05$), with the lowest value of 24.13 ± 0.58 discovered in beef aged for 7 days. When compared to the non-ultrasonic group, the shear force of the ultrasonic group was significantly ($p<0.05$) lower in the control group.

The water-holding capacity (WHC) was evaluated by measuring pressure loss and cooking loss to characterize juiciness in this study (Huff-Lonergan and Lonergan, 2005). The results showed that as the aging time increased, pressure loss significantly increased from 36.25 % to 45.62 % ($p<0.05$), indicating that aging contributed to an increased in the WHC. Additionally, the results indicated that the pressure loss and cooking loss of the ultrasonic group were significantly lower than that of the non-ultrasonic group. This suggested that ultrasound could significantly reduce pressure loss and free water content during cooking of beef while increasing immobilized water content. Meanwhile, it indicated that the WHC of the ultrasonic sample was higher than that of the non-ultrasonic group. The reduction of pH value and the process of rigidity will also lead to the contraction of myofibril, consequently decreasing the space for water storage and increasing water loss.

3.2. Changes in myofibrillar fragmentation index

The myofibrillar fragmentation index (MFI) reflects the extent of disintegration of muscle fibers and their skeletal proteins, which is widely used for the evaluation of meat tenderness. Table S2 illustrated a significant effect on MFI caused by both ultrasound treatment and aging time ($p<0.05$), which was consistent with that of the hardness. The results showed that the ultrasonic group showed a significantly higher MFI value ($p<0.05$) compared to the non-ultrasonic group. Meanwhile, with the prolonged aging time, the MFI values of different samples demonstrated an upward trend, indicating that aging could effectively improve the tenderness by fragmentation of myofibrils. Therefore, ultrasound had an effective effect on enhancing the tenderness of the beef *longissimus lumborum*.

3.3. Immunoblotting analysis of desmin and caspase-3

Desmin is an important cytoskeleton protein in muscle cells, which may be the key substrate that determines meat tenderness. Fragmentation of desmin was observed within 7 days after slaughter, thus proving that ultrasound treatment resulted in a significant decrease in strip strength, which was consistent with the results of MFI. It is noteworthy that caspase-3 exists initially as a precursor molecule with a molecular weight of approximately 32 kDa. The levels of caspase-3 were decreased in beef aged for 3 days and 7 days compared to that immediately after slaughter (Fig. 1). In this work, we discovered that the expression of caspase-3 was increased by ultrasound treatment. The western blot bands of caspase-3 with ultrasound were significantly weaker during 3 days compared to the control group, indicating that ultrasound significantly increased the level of caspase-3, which can promote cell apoptosis during muscle tenderization. Chen et al. (2021) discovered that applying ultrasound treatment at a frequency of 40 kHz and intensity of 1500 W can significantly increase the activities of desmin and caspase-3 in chicken muscle after slaughter. It was believed that ultrasound influenced meat aging via possibly activated myofibril degradation and apoptosis. The results indicated that the improvement in the tenderness of the *longissimus lumborum* by ultrasound treatment was due to the increased caspase-3 activity (Dang et al., 2022).

3.4. Changes in proteome profiles during aging

The mass spectrometry proteomics data have been deposited to the ProteomeXchange Consortium (https://proteomecentral.proteomexchange.org/cgi/GetDataset?ID=PXD050302).

In this investigation, *longissimus lumborum* subjected to ultrasound was evaluated for protein expression and proteome distinctions using label-free analysis. A total of 1482 proteins were identified, along with 1298 proteins shared by both groups, shown in Fig. S1(A). Furthermore, the logarithm of all protein fold changes was used as the ordinate to plot a scatter plot (Fig. S1(B)). Differentially expressed proteins were filtered out for additional analysis in order to more accurately compare the proteome differences between the ultrasonic and non-ultrasonic groups. 47 differentially expressed proteins were identified with FC > 1.5 or < 0.6667 ($p<0.05$) in CK vs. US, which were summarized in Table S3, including 27 down-regulated and 20 up-regulated proteins (Fig. S1(C)).

The effect of ultrasound on meat proteins that exhibited differential expression was identified via the PCA analysis on 47 proteins (Table S3). In the score chart (Fig. S2(A)), the results of PCA demonstrated that the first two principal components covered 85.3 % of the total data variation (PC1 and PC2), which accounted for 69.7 % and 15.6 %, respectively. PC1 distinguished the samples in the US from CK. The protein profile of beef *longissimus lumborum* experienced alterations following ultrasonic treatment, as indicated by the results.

HCA was used to determine the proteomics difference between non-ultrasonic and ultrasonic samples after 1 day of aging. The resulting heat map analysis of the 47 proteins with differentially expressed levels revealed the modifications (Fig. S2(B)). The data were represented graphically by the HCA diagram, each point representing a change of protein content. As the quantity of proteins with differentially expressed levels increased, the colour scale shifted from blue to red. Distinct colour distributions were observed between the groups subjected to ultrasound and those not, elucidating noteworthy alterations in the proteome subsequent to the application of ultrasound. Due to the increase of Euclidean distance, non-ultrasonic and ultrasonic samples were collected separately in different clusters. This suggested that noteworthy distinctions were present among variable samples, a finding that was consistent with the results of PCA analysis.

The PLS-DA model was conducted to further classify and explain markers in the observed protein profiles of the non-ultrasonic and ultrasonic samples (Jia et al., 2021). PLS-DA analysis was used in this work to successfully separate samples with various treatments, and the classification outcomes were consistent with those of the unsupervised PCA method. According to Fig. S2(C), there was a significant difference between no treatment and ultrasound samples ($R^2 = 0.991$ and $Q^2 =$

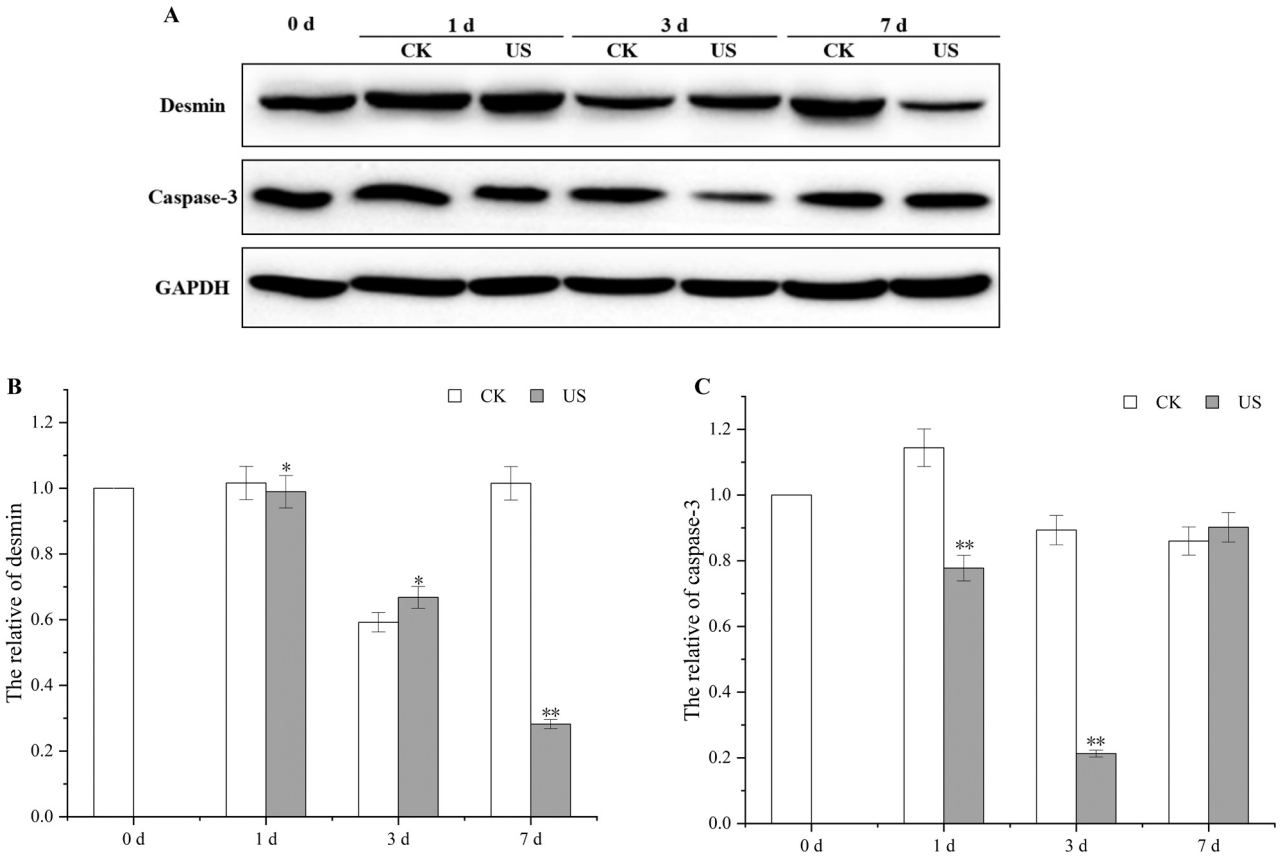

Fig. 1. (A) Immunoblotting analysis of desmin and caspase-3 in beef muscle treated with or without ultrasound. (B) The grayscale value of desmin. (C) The grayscale value of caspase-3. **: $p<0.01$ vs. CK. *: $p<0.05$ vs. CK.

Table 1
Differentially expressed proteins of beef with VIP > 1 at 1 d of aging ($P < 0.05$).

Protein ID	Protein names	Gene names	VIP scores	Fold-change	
				US/CK	*P*-value
Q3SYU7	Transportin-1	TNPO1	1.2	0.0771	0
P01252	Prothymosin alpha	PTMA	1.1975	7.5164	0
P33672	Proteasome subunit beta type-3	PSMB3	1.1883	0.2821	0.0001
Q3SZV7	Hemopexin	HPX	1.184	1.8799	0.0033
A0A3Q1LJU5	EMAP like 2	EML2	1.1837	0.0821	0.0002
Q8MKH6	Troponin T, slow skeletal muscle	TNNT1	1.1822	1.74	0.0042
A0A3Q1MFN5	Troponin T, slow skeletal muscle	TNNT1	1.1822	1.74	0.0042
P01966	Hemoglobin subunit alpha	HBA	1.1772	1.5513	0.0152
A0A3Q1MG04	Fibrinogen beta chain	FGB	1.1766	1.8095	0.0113
P12763	Alpha-2-HS-glycoprotein	AHSG	1.1728	1.9632	0.0096
P02070	Hemoglobin subunit beta	HBB	1.1692	1.5247	0.0196
Q3MIC0	60 S ribosomal protein L37a	RPL37A	1.1689	7.1334	0.0013
A0A3Q1ME08	Titin		1.1674	3.8913	0.0097
Q3SWX4	Glioblastoma amplified sequence	NIPSNAP2	1.1615	1.7689	0.0098
A6QQ09	LOC100138230 protein (Fragment)	LOC100138230	1.1569	0.0878	0.0025
A0A3Q1LT19	Ig-like domain-containing protein		1.1538	17.8667	0.0031
P00125	Cytochrome c1, heme protein, mitochondrial	CYC1	1.1507	1.8648	0.0294
A0A3Q1LPR0	Heterogeneous nuclear ribonucleoprotein A3		1.1483	12.8907	0.0033
A0A3Q1MGF6	Ryanodine receptor 2	RYR2	1.1386	1.8295	0.019
A0A3Q1M3I6	Serine/threonine-protein phosphatase 2A 55 kDa regulatory subunit B	PPP2R2A	1.1236	0.1139	0.0048
A0A3Q1LGL7	Laminin subunit alpha 4	LAMA4	1.1097	0.1207	0.0077
O97680	Thioredoxin	TXN	1.1044	1.7086	0.0427
Q17Q89	Prefoldin subunit 6	PFDN6	1.1011	0.206	0.002
P34942	NADH dehydrogenase [ubiquinone] 1 alpha subcomplex subunit 10, mitochondrial	NDUFA10	1.1007	2.747	0.0206
A7YWQ4	SNTB2 protein	SNTB2	1.0966	4.0958	0.0227
Q3T0F4	40S ribosomal protein S10	RPS10	1.0874	2.914	0.0424
Q3SWZ6	Ribosome maturation protein SBDS	SBDS	1.0112	0.1814	0.0135
G3N016	CRK like proto-onco, adaptor protein	CRKL	1.0107	5.2149	0.0498

Note: Protein abundance was exceeded by fold-changes (ratio > 1.5 or < 0.6667).

0.951). Values Importance in Projection (VIP) scores for proteins contributing to the ultrasonic treatment of beef *longissimus lumborum* were assessed. A total of 28 proteins were obtained with VIP value > 1 as the screening condition, as shown in Fig. S2(D). Among them, 20 proteins (Q3T0E0, P34942, A03Q1ME08, A0A3Q1LPR0, O97680, A0A3Q1MG04, Q3MIC0, Q3SZV7, Q3SWX4, A0A3Q1LT19, P01252, A0A3Q1MFN5, Q8MKH6, P00125, G3N016, A0A3Q1MGF6, P12763, P01966, A7YWQ4, and P02070) had high content in the ultrasonic sample, while 8 proteins (A0A3Q1LJU5, Q3SYU7, P33672, A6QQ09, A0A3Q1M3I6, A0A3Q1LGL7, Q3SWZ6, and Q17Q89) had obvious changes in the non-ultrasonic sample. As shown in Table 1, the differentially expressed proteins that VIP value > 1 were listed, and the content of all proteins increased following ultrasonic treatment. Further screening of proteins related to meat tenderness changes.

3.5. Analysis of tenderness-related proteins

PCA was conducted to more clearly illustrate the relationships between the 28 significant proteins and the two factors that affect beef tenderness (Shear force and MFI), as shown in Fig. 2. The results of PCA demonstrated that first two principal components covered 91.3 % of the total data variation and effectively separated different groups. Most of the variation (84.7 %) accounted for PC1. A0A3Q1LJU5, Q3SYU7, P33672, A6QQ09, A0A3Q1M3I6, A0A3Q1LGL7, Q3SWZ6, and Q17Q89, as well as hardness scores, were negatively connected with PC1 and positively correlated with all other proteins projected by MFI values, including Q3T0E0, P34942, A03Q1ME08, A0A3Q1LPR0, O97680, A0A3Q1MG04, Q3MIC0, Q3SZV7, Q3SWX4, A0A3Q1LT19, P01252, A0A3Q1MFN5, Q8MKH6, P00125, G3N016, A0A3Q1MGF6, P12763, P01966, A7YWQ4, and P02070. The PC2 accounted for a slight variation of approximately 6.6 %. Troponin T, slow skeletal muscle (Q8MKH6, A0A3QQ1MFN5) was more prevalent in the ultrasonic sample than in the control (FC=1.74). In addition, studies have shown that the breakdown of Troponin T and the disruption of contacts with other filaments result in the breakage of filaments in zone I, which may cause myofibril to rupture or potentially compromise the structural integrity of the entire muscle (Zhang et al., 2020). According to the results, the improvement of tenderness after 1 day of aging may not be related to the degradation of Troponin T. Ryanodine receptor 2 (RYR2) mediates the flow of calcium ions and may affect beef tenderness. The results suggested that ultrasound treatment improved beef tenderness at 1 day of aging, as indicated by the up-regulation of thioredoxin. Thioredoxin (O97680) is known to regulate intracellular redox status and protect against oxidative stress damage. Additionally, it can modulate caspase-3 activity through its nitrosylation active site. Downregulation of Serine/threonine-protein phosphatase 2 A (PPP2R2A) verified the same result due to its inhibitory effect on apoptosis. The ultrasound treatment suppressed its synthesised, which eventually led to an increase in tenderness.

3.6. Bioinformatics analysis of the differential proteins

Bioinformatics analysis is a method of analyzing a large number of genes or their transcripts and annotating the functionality of a dataset to obtain interpretable discoveries and viewpoints in biology. It has been effectively applied to proteomics and was created for processing different forms of biological data (Kumar and Mann, 2009). In this study, three bioinformatics methods were used to in-depth excavate the

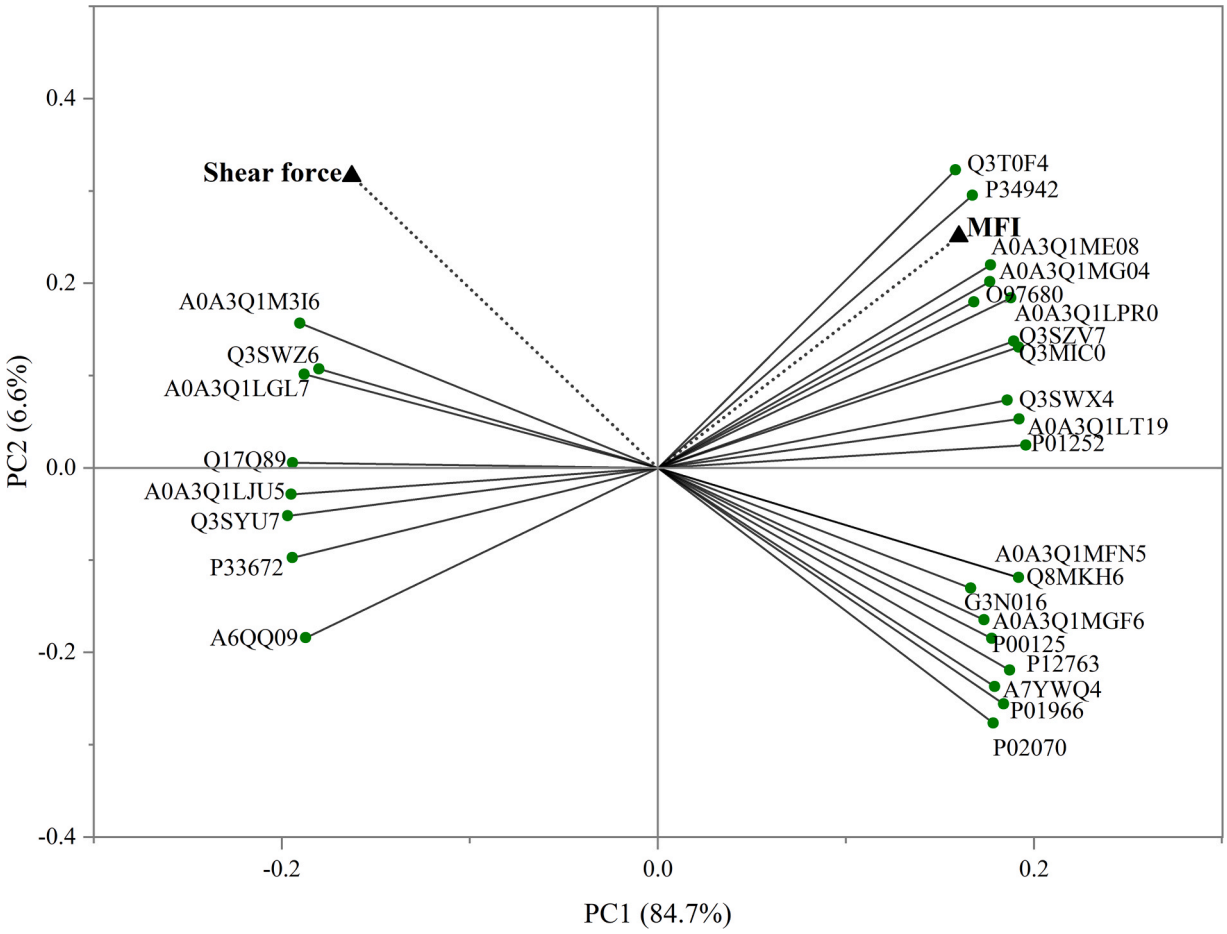

Fig. 2. Projection of proteins among two tenderness-related parameters (Shear force and MFI).

information of differentially expressed proteins affected by ultrasound processing: Gene Ontology analysis, subcellular localization analysis, and protein-protein interaction analysis. A quantitative analysis of 47 differentially expressed proteins was conducted to investigate the relevance, functional categorization, and correlation of differentially expressed proteins in GO functional project analysis. As for biological process, differentially expressed proteins were primarily associated with cellular, regulation, and metabolic processes (Fig. 3(A)). In the plot of the cell component, differentially expressed proteins were mainly involved in the cellular anatomical entity and protein-containing complex. Molecular function analysis showed that most differentially expressed proteins were related to the functions of binding proteins and catalytic activity. Binding protein is considered an important factor affecting the muscle organizational framework, which can maintain internal balance, regulate muscle relaxation or contraction, promote the assembly of myosin bundles, and provide physical protection against environmental stress (Purslow et al., 2021). In muscle cells, the catalytic activity is closely related to the rate of various biochemical reactions. The subcellular localization analysis (Fig. 3(B)) indicated that the cytoplasm (GO:0005737), membrane (GO:0016020), and endoplasmic reticulum (GO:0005783) were the primary subcellular locations, accounting for 52.24 %, 16.42 %, and 7.46 %, respectively.

The KEGG enrichment results of the proteomics for up-regulated and down-regulated proteins yielded six common KEGG pathways as shown in Fig. 3(C). The blue column represented the pathway enriched by down-regulated proteins, while the red column represented the pathway enriched by up-regulated proteins. Four of the six pathways were related to the metabolism, including selenocompound metabolism, oxidative phosphorylation, tryptophan metabolism and cysteine and methionine metabolism. The oxidative phosphorylation pathway was associated with tenderness. What's more, the differential proteins involved in this pathway were CYC1 (P00125) and NADUFA10 (P34942). In the hypoxia that followed slaughter, CYC1 entered cells and mitochondria and was involved in collagen formation and apoptosis, affecting the tenderness of beef. The up-regulation of NDUFA10 could enhance the anaerobic glycolysis pathway, leading to an increase in the production of pyruvic acid. This increase in pyruvic acid production could result in a decrease in pH, which promotes proteolysis and ultimately leads to increased meat tenderness.

To gain further bioinformatics information, the protein-protein interaction networks of all discovered differentially expressed proteins affected by ultrasound were acquired from String 11.5. According to Fig. 4, the PPI network depicts the interrelationships between proteins that are expressed differently. The proteins (AHSG, TGB, CRKL, RHOA, STRN3, NDUFA10, and CYC1) that were located in the cytoplasm and membrane were strongly connected with each other. Among these,

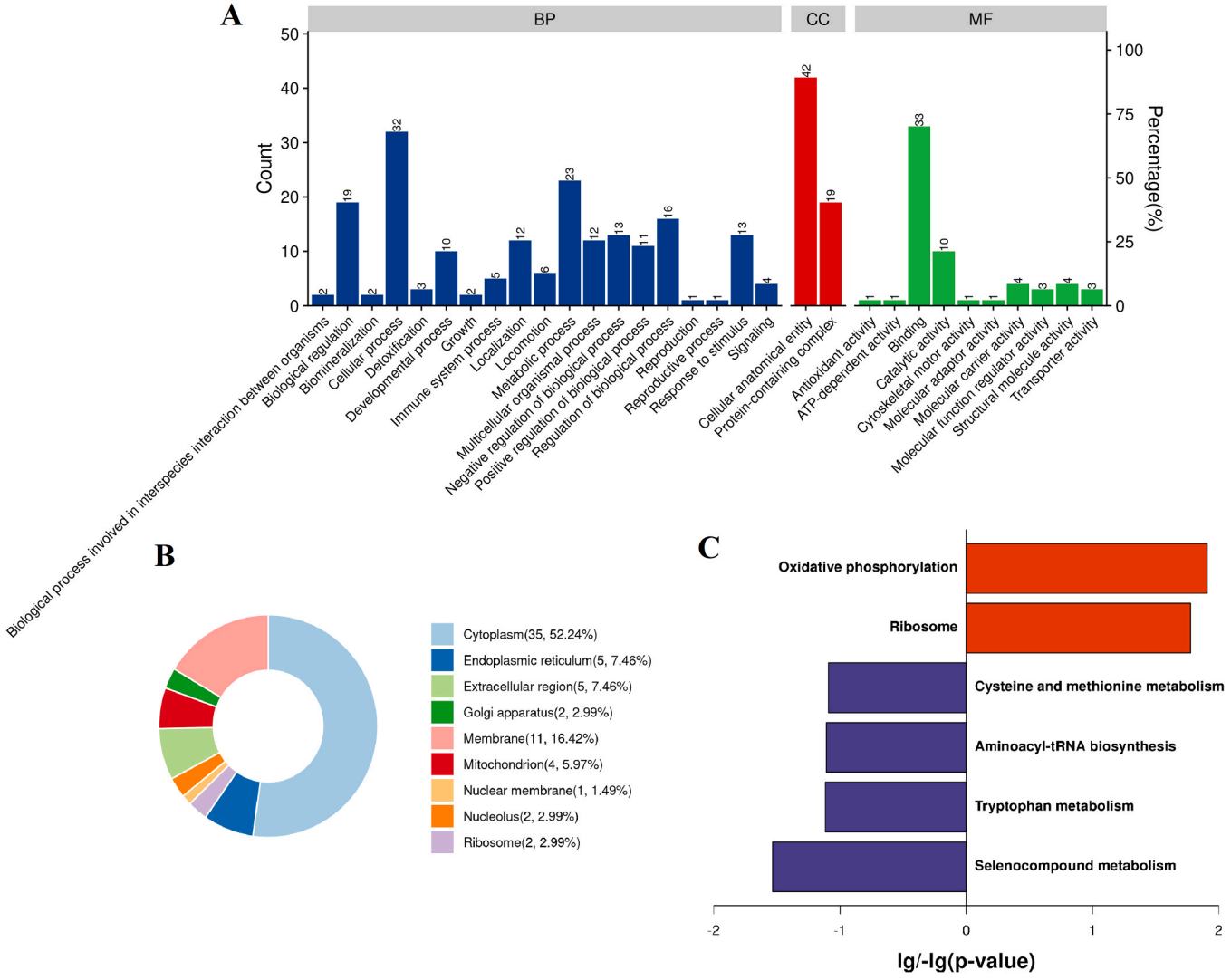

Fig. 3. GO annotation classification (A), subcellular localization analysis (B) and KEGG pathways (C) of differentially expressed proteins between the non-ultrasonic and ultrasonic groups.

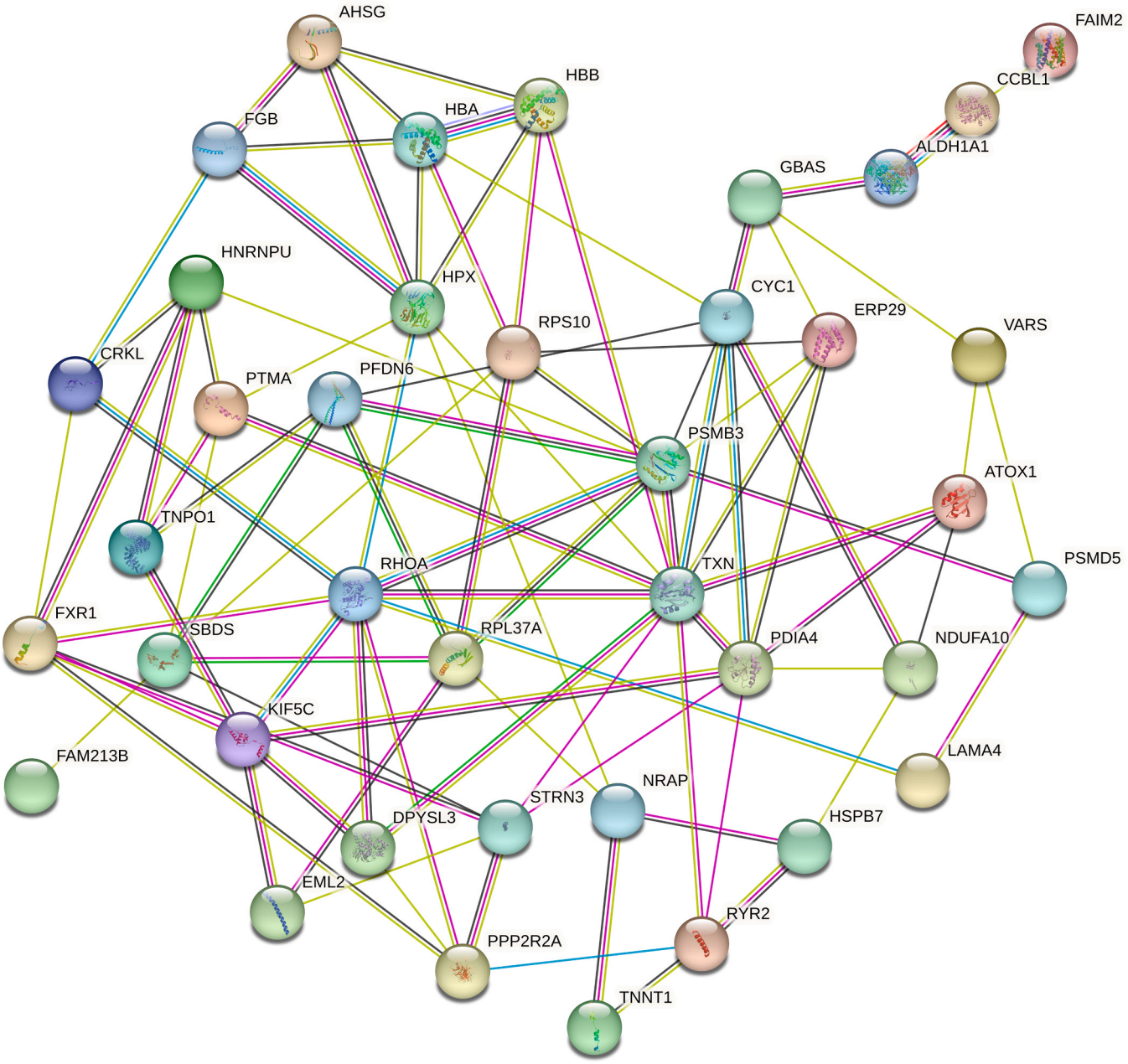

Fig. 4. PPI network of the total differentially expressed proteins.

CYC1 and NADUFA10 were presented in mitochondrion. The proteins distributed in the nucleolus (SBDS, RPS10) and those dispersed in the endoplasmic reticulum (FGB, RYR2, ERP29, PDIA4) interacted closely. These findings supported the distribution of differently expressed proteins, which proved the hypothesis that ultrasonic mostly affected the proteins situated in the cytoplasm, membrane, and nucleus.

4. Conclusion

Muscle cells experience hypoxia and ischemia after animal slaughter, leading to apoptosis. Our findings suggested that ultrasound can induce the morphological characteristics of nuclei and apoptotic mitochondria during postmortem aging. Ultrasound treatment during postmortem aging of 7 days reduced the beef's hardness and caused the breaking of desmin fragments, suggesting an improvement in tenderness quality from ultrasound treatment. The study into meat tenderization and potential mechanism of muscle conversion in the Simmental cattle breed allowed to conclude that their meat can be judged tender after 7 days of aging. From the analysis of proteomics data, the protein mass spectrometry was altered by ultrasound treatment at 1 day of aging. Most of the 47 differentially expressed proteins screened out showed higher discrimination. The cytoplasm, membrane, and nucleus included the differently expressed proteins that were more sensitive to ultrasound. In addition, 28 proteins (FC > 1.5, VIP > 1) might be potential markers for tenderness. All these findings provided new insight into the impact of ultrasound on meat protein changes and tenderness, and laid a foundation for understanding proteomics in the early stages of meat aging. The improvement in tenderness of beef in late maturation requires further in-depth studies.

CRediT authorship contribution statement

Xiuyun Guo: Software, Methodology. **Rui Liu:** Software, Methodology. **Anqi Xu:** Formal analysis, Data curation. **Chuanming Huan:**

Software, Data curation. **Zhicheng Xu:** Validation, Formal analysis. **Hengpeng Wang:** Writing – review & editing, Project administration, Funding acquisition. **Sumin Gao:** Writing – review & editing, Writing – original draft, Methodology, Data curation. **Xiangren Meng:** Writing – review & editing, Funding acquisition, Formal analysis, Conceptualization. **Peng Wu:** Validation, Formal analysis.

Declaration of Competing Interest

The authors declare that they have no known competing financial interests or personal relationships that could have appeared to influence the work reported in this paper.

Data availability

Data will be made available on request.

Acknowledgments

The research was finally supported by the Chinese Nutrition Society - Baisheng Catering Health Fund (grant number CNS-YUM2020A17), the Social Science Foundation of Jiangsu Province (grant number 17GLD021), the Qinglan Project of Yangzhou University (grant number 137050358), the 2022 Supported Project of Cuisine Science Key Laboratory of Sichuan Province (grant number PRKX2022Z15), and the Leading Talent Funding Project of "Lv Yang Jinfeng plan" in Yangzhou. We also appreciated the technical support provided by Shanghai Bioprofile Technology Co., Ltd.

Appendix A. Supporting information

Supplementary data associated with this article can be found in the online version at doi:10.1016/j.jfca.2024.106220.

References

Ashburner, M., Ball, C.A., Blake, J.A., Botstein, D., Butler, H., Cherry, J.M., Sherlock, G., 2000. Gene ontology: tool for the unification of biology. Nat. Genet. 25 (1), 25–29.
Barekat, S., Soltanizadeh, N., 2018. Effects of ultrasound on microstructure and enzyme penetration in beef LL muscle. Food Bioprocess Technol. 11, 680–693.
Bax, M.L., Sayd, T., Aubry, L., Ferreira, C., Viala, D., Chambon, C., Santé-Lhoutellier, V., 2013. Muscle composition slightly affects in vitro digestion of aged and cooked meat: identification of associated proteomic markers. Food Chem. 136 (3-4), 1249–1262.
Bonnet, M., Soulat, J., Bons, J., Léger, S., De Koning, L., Carapito, C., Picard, B., 2020. Quantification of biomarkers for beef meat qualities using a combination of parallel reaction monitoring-and antibody-based proteomics. Food Chem. 317, 126376.
Brewer, S., Novakofski, J., 2008. Consumer sensory evaluations of aging effects on beef quality. J. Food Sci. 73 (1), S78–S82.
Chen, L., Chai, Y., Luo, J., Wang, J., Liu, X., Wang, T., Feng, X., 2021. Apoptotic changes and myofibrils degradation in post-mortem chicken muscles by ultrasonic processing. LWT-Food Sci. Technol. 142, 110985.
Culler, R.D., Parrish, F.C., Jr, Smith, G.C., Cross, H.R., 1978. Relationship of myofifibril fragmentation index to certain chemical, physical, and sensory characteristics of bovine longissimus muscle. Food Sci. 43, 1177.
Dang, D.S., Stafford, C.D., Taylor, M.J., Buhler, J.F., Thornton, K.J., Matarneh, S.K., 2022. Ultrasonication of beef improves calpain-1 autolysis and caspase-3 activity by elevating cytosolic calcium and inducing mitochondrial dysfunction. Meat Sci. 183, 108646.
Goll, D.E., Thompson, V.F., Li, H., Wei, W., Cong, J., 2003. The calpain system. Physiol. Rev. 83 (3), 731–801.
González-González, L., Luna-Rodríagez, L., Carrillo-López, L.M., Alarcón-Rojo, A.D., García-Galicia, I.A., Reyes-Villagrana, R., 2017. Ultrasound as an alternative to conventional marination: acceptability and mass transfer. J. Food Qual., 86757209
Herrera-Mendez, C.H., Becila, S., Boudjellal, A., Ouali, A., 2006. Meat ageing: Reconsideration of the current concept. Trends Food Sci. Technol. 17 (8), 394–405.
Holman, B.W.B., Alvarenga, T.I.R.C., van de Venc, R.J., Hopkin, D.L., 2015. A comparison of technical replicate (cuts) effect on lamb Warner-Bratzler shear force measurement precision. Meat Sci. 105, 93–95.
Hou, X., Liu, Q., Meng, Q., Wang, L., Yan, H., Zhang, L., Wang, L., 2020. TMT-based quantitative proteomic analysis of porcine muscle associated with postmortem meat quality. Food Chem. 328, 127133.
Huang, C., Hou, C., Ijaz, M., Yan, T., Li, X., Li, Y., Zhang, D., 2020. Proteomics discovery of protein biomarkers linked to meat quality traits in post-mortem muscles: current trends and future prospects: a review. Trends Food Sci. Technol. 105, 416–432.
Huff-Lonergan, E., Lonergan, S.M., 2005. Mechanisms of water-holding capacity of meat: the role of postmortem biochemical and structural changes. Meat Sci. 71 (1), 194–204.
Huff-Lonergan, E., Zhang, W., Lonergan, S.M., 2010. Biochemistry of postmortem muscle—lessons on mechanisms of meat tenderization. Meat Sci. 86 (1), 184–195.
Jia, W., Zhang, R., Liu, L., Zhu, Z., Xu, M., Shi, L., 2021. Molecular mechanism of protein dynamic change for Hengshan goat meat during freezing storage based on high-throughput proteomics. Food Res. Int. 143, 110289.
Kim, Y.H.B., Ma, D., Setyabrata, D., Farouk, M.M., Lonergan, S.M., Huff-Lonergan, E., Hunt, M.C., 2018. Understanding postmortem biochemical processes and post-harvest aging factors to develop novel smart-aging strategies. Meat Sci. 144, 74–90.
Kim, Y.H.B., Warner, R.D., Rosenvold, K., 2014. Influence of high pre-rigor temperature and fast pH fall on muscle proteins and meat quality: a review. Anim. Prod. Sci. 54 (4), 375–395.
Kumar, C., Mann, M., 2009. Bioinformatics analysis of mass spectrometry-based proteomics data sets. FEBS Lett. 583 (11), 1703–1712.
Li, M., Zhang, D., Chai, W., Zhu, M., Wang, Y., Liu, Y., Wang, C., 2022. Chemical and physical properties of meat from Dezhou black donkey. Food Sci. Technol. Res. 28 (1), 87–94.
Li, G., Li, Z., Li, X., Wang, Y., Zhu, J., Zhang, D., 2019. Postmortem ageing influences the thawed meat quality of frozen lamb loins. Food Chem. 275, 105–112.
López-Pedrouso, M., Lorenzo, J.M., Di Stasio, L., Brugiapaglia, A., Franco, D., 2021. Quantitative proteomic analysis of beef tenderness of Piemontese young bulls by SWATH-MS. Food Chem. 356, 129711.
Malheiros, J.M., Braga, C.P., Grove, R.A., Ribeiro, F.A., Calkins, C.R., Adamec, J., Chardulo, L.A.L., 2019. Influence of oxidative damage to proteins on meat tenderness using a proteomics approach. Meat Sci. 148, 64–71.
Montowska, M., Pospiech, E., 2013. Species-specific expression of various proteins in meat tissue: proteomic analysis of raw and cooked meat and meat products made from beef, pork and selected poultry species. Food Chem. 136 (3-4), 1461–1469.
Peña-González, E.M., Alarcón-Rojo, A.D., Rentería, A., García, I., Santellano, E., Quintero, A., Luna, L., 2017. Quality and sensory profile of ultrasound-treated beef. Ital. J. Food Sci. 29 (3).
Picard, B., Gagaoua, M., 2020. Meta-proteomics for the discovery of protein biomarkers of beef tenderness: An overview of integrated studies. Food Res. Int. 127, 108739.
Purslow, P.P., Gagaoua, M., Warner, R.D., 2021. Insights on meat quality from combining traditional studies and proteomics. Meat Sci. 174, 108423.
Sarabandi, K.H., Peighambardoust, S.H., Sadeghi Mahoonak, A.R., Samaei, S.P., 2018. Effect of different carriers on microstructure and physical characteristics of spray dried apple juice concentrate. J. Food Sci. Technol. 55, 3098–3109.
Shi, J., Zhang, L., Lei, Y., Shen, H., Yu, X., Luo, Y., 2018. Differential proteomic analysis to identify proteins associated with quality traits of frozen mud shrimp (Solenocera melantho) using an iTRAQ-based strategy. Food Chem. 251, 25–32.
Stadnik, J., Dolatowski, Z.J., Baranowska, H.M., 2008. Effect of ultrasound treatment on water holding properties and microstructure of beef (m. semimembranosus) during ageing. LWT-Food Sci. Technol. 41 (10), 2151–2158.
Tyanova, S., Temu, T., Sinitcyn, P., Carlson, A., Hein, M.Y., Geiger, T., Cox, J., 2016. The Perseus computational platform for comprehensive analysis of (prote) omics data. Nat. Methods 13 (9), 731–740.
Wang, A., Kang, D., Zhang, W., Zhang, C., Zou, Y., Zhou, G., 2018. Changes in calpain activity, protein degradation and microstructure of beef M. semitendinosus by the application of ultrasound. Food Chem. 245, 724–730.
Wiśniewski, J.R., Zougman, A., Nagaraj, N., Mann, M., 2009. Universal sample preparation method for proteome analysis. Nat. Methods 6 (5), 359–362.
Zhang, M., Xia, X., Liu, Q., Chen, Q., Kong, B., 2019. Changes in microstructure, quality and water distribution of porcine longissimus muscles subjected to ultrasound-assisted immersion freezing during frozen storage. Meat Sci. 151, 24–32.
Zhang, Y.Y., Zhang, D.J., Huang, Y.J., Chen, L., Bao, P.Q., Fang, H.M., Zhou, C.L., 2020. L-arginine and L-lysine degrade troponin-T, and L-arginine dissociates actomyosin: their roles in improving the tenderness of chicken breast. Food Chem. 318, 126516.